

Zeitschrift: Helvetica Physica Acta
Band: 58 (1985)
Heft: 2-3

Artikel: Theory of localized defects in semiconductors
Autor: Schlüter, M.
DOI: <https://doi.org/10.5169/seals-115605>

Nutzungsbedingungen

Die ETH-Bibliothek ist die Anbieterin der digitalisierten Zeitschriften auf E-Periodica. Sie besitzt keine Urheberrechte an den Zeitschriften und ist nicht verantwortlich für deren Inhalte. Die Rechte liegen in der Regel bei den Herausgebern beziehungsweise den externen Rechteinhabern. Das Veröffentlichen von Bildern in Print- und Online-Publikationen sowie auf Social Media-Kanälen oder Webseiten ist nur mit vorheriger Genehmigung der Rechteinhaber erlaubt. [Mehr erfahren](#)

Conditions d'utilisation

L'ETH Library est le fournisseur des revues numérisées. Elle ne détient aucun droit d'auteur sur les revues et n'est pas responsable de leur contenu. En règle générale, les droits sont détenus par les éditeurs ou les détenteurs de droits externes. La reproduction d'images dans des publications imprimées ou en ligne ainsi que sur des canaux de médias sociaux ou des sites web n'est autorisée qu'avec l'accord préalable des détenteurs des droits. [En savoir plus](#)

Terms of use

The ETH Library is the provider of the digitised journals. It does not own any copyrights to the journals and is not responsible for their content. The rights usually lie with the publishers or the external rights holders. Publishing images in print and online publications, as well as on social media channels or websites, is only permitted with the prior consent of the rights holders. [Find out more](#)

Download PDF: 01.07.2025

ETH-Bibliothek Zürich, E-Periodica, <https://www.e-periodica.ch>

Theory of localized defects in semiconductors

M. Schlüter, AT&T Bell Laboratories, Murray Hill, New Jersey
07974

(28. VI. 1984)

In honor of Emanuel Mooser's 60th birthday

Abstract. The combination of Density Functional Theory and Pseudopotential Theory has been successfully applied to the description of point-defects in semiconductors. Characteristic features of such defects are that local electronic states couple strongly to local lattice distortions and exhibit sizeable Coulomb interaction effects. This can lead to exotic features such as “negative U ” behavior and electronically enhanced atomic migration.

I. Introduction

The electronic and structural properties of defects in semiconductors, are of continued strong interest. Defects or impurities, even in small quantities, strongly influence device performance, either by creating certain desired performance properties or conversely by accidentally degrading them. Additionally, there is the basic theoretical challenge itself to describe the physics of defects. This latter argument applies notably to localized or “deep-level” defects which I shall consider here.

The particular difficulties that are associated with the description of deep defects are, among others, the intermediate range of localization of the defect-induced perturbation and the strong coupling between localized electronic and vibronic states. While difficult to describe theoretically, it has become clear that these properties are directly responsible for a large number of particular and interesting physical properties, such as e.g. negative effective electron–electron correlation effects and recombination enhanced defect migration.

There are strong analogues between effects occurring on solid surfaces, e.g. reconstructions or chemisorption processes, and the local chemistry occurring near defects. The similarities have traditionally had an influence on the approaches developed by theorists to describe defects. I shall discuss here a particularly successful approach, the combination of Density Functional Theory and Pseudopotential Theory within the Green's function framework.

II. Formulation of the problem

To describe a localized defect we first consider a perfect, translationally invariant, infinite semiconductor crystal. A point defect is created by e.g., removing one crystal atom, or replacing it by an impurity atom or by similar operations. We define a small region of action around the defect in which *strong* chemical

effects occur. These effects are e.g., the formation of dangling bonds leading to undercoordinated atoms near a vacancy or conversely the attempt to form new bonds between an extra interstitial atom and its overcoordinated neighbors or simply the modification of the strength of bonds around a substitutional impurity. In general, atoms in this region will distort significantly from their original perfect crystal position. In semiconductors, this region is typically a few screening lengths ($\approx 5\text{--}10\text{\AA}$) in diameter and contains of the order of 20–40 atoms. The region of *action* is surrounded by a much larger region of *reaction* over which the crystal's response to the defect can best be described by elastic and dielectric means. The point is, that small distortions and polarizations persist in principle up to infinite range without significant perturbations on a local scale.

The complexity of the problem can be further illustrated by considering, in addition to the different length scales mentioned above, the role of different energy scales. The largest energy in the problem is of chemical nature, often called “central-cell” potential and describes the difference in atomic structure between e.g., the impurity atom and the host atom. The strength of this potential ranges from $<1\text{ eV}$ to several 10 eV depending on the relative position of impurity and host in the periodic table. Next is the energy associated with the formation of bonds, typically of the order of a few eV. Since defects in semiconductors can create localized electronic states (i.e., the deep levels in the gap) Coulomb effects are of importance. The Coulomb contributions range from $\sim 0.1\text{ eV}$ to $\sim 0.5\text{ eV}$ which is compatible with semiconductor screening and an approximate wave function localization over $5\text{--}10\text{ \AA}$. Finally, large lattice distortion energies occur up to $\sim 0.5\text{ eV}$, mainly resulting from short range contributions. The important point to note here is that both Coulomb repulsion and lattice distortion energies depend strongly on the defect *charge state*, i.e., on the number of electrons trapped at the defect site. Trapping and detrapping can thus be accompanied by large energy releases coupled to atomic motions with amplitudes up to several tenths of \AA . All energy scales mentioned have to be compared to the value of the semiconductor energy gap which is of the order of 1 eV and which is the “experimental window” for defect spectroscopy.

The task to deal with these problems can be separated into two categories: first, how to describe the atomic arrangement and second, how to account for the strong chemical changes around the defect. The number of approaches to handle these problems is large. We shall here, discuss the Green's function approach which represents a formal and practical way to calculate the properties of a defect which is embedded in a perfect crystal. To describe the chemical changes and interactions we will use the Density Functional approach and first-principles pseudopotentials.

III. Theoretical tools

a) The Density Functional Theory integrates the lattice ion-potential V_{ext} with the mutual interaction of electrons. The theory is based on the theorem by Hohenburg and Kohn [1] which states that all properties of the many particle ground state are given by the ground state electron *density* distribution. The solution of the many-body ground state is thus reduced exactly to the solution for the ground state density. In this way the energy of a system of interacting

electrons in an external nuclear potential can be written as

$$E[\rho] = T[\rho] + E_{\text{coul}}[\rho] + \int V_{\text{ext}}(r)\rho(r) dr + E_{\text{xc}}[\rho] \quad (1)$$

where $T[\rho]$ is the kinetic energy of the *non-interacting* electrons,

$$E_{\text{coul}}[\rho] = \frac{1}{2} \int \frac{\rho(r)\rho(r')}{|r-r'|} dr dr',$$

the usual Coulomb energy, where the electrons are treated as fixed and “uncorrelated”, $V_{\text{ext}} = -Z/r$, the nuclear potential, and $E_{\text{xc}}[\rho]$ the exchange correlation energy, which globally contains all interactions due to the Pauli exclusion principle and to the otherwise correlated motion of electrons. As shown by Kohn and Sham [2], a variation solution of equation (1) can be obtained by solving a set of one-electron Schrödinger-type equations self-consistently:

$$[T + V(r)]\psi_i(r) = \epsilon_i \psi_i(r)$$

with

$$V(r) = \int \frac{\rho(r')}{|r-r'|} dr' + \frac{\delta E_{\text{xc}}[\rho]}{\delta \rho(r)} + V_{\text{ext}}(r) \quad (2)$$

and

$$\rho(r) = \sum_{\text{occupied states}} |\psi_i(r)|^2$$

The occupation of the states $\psi_i(r)$ is done according to Fermi statistics with the eigenvalue ϵ_i serving as the energy for the purpose of determining occupancy of a state. The solution of the many-body problem is thus reduced to the solution of a set of one-particle equations, not more difficult to solve than the Hartree problem. The difficulty lies in determining the unknown functionals $E_{\text{xc}}[\rho]$ and $V_{\text{xc}}[\rho] = \delta E_{\text{xc}}[\rho]/\delta \rho(r)$. Here an important concept yields the framework for practical approximations. In analogy to the Thomas–Fermi methods, an approximation (Local Density Functional) to E_{xc} and V_{xc} is given by regarding a small neighborhood of the electron system as behaving like jellium i.e., $\rho = \text{const}$, at the value of the local density. Then $E_{\text{xc}}[\rho] \approx \int \rho(r) E_{\text{xc}}^h[\rho(r)] dr$ and well-known approximations for the homogeneous electron gas exchange–correlation energies E_{xc}^h can be used. Discussions on various aspects of density functional theory can be found in several recent reviews [3–6].

b) Pseudopotentials were originally introduced to simplify electronic structure calculations by eliminating the need to include atomic core states and the strong potentials responsible for binding them. Considerable success was achieved in describing the band structure and optical properties of semiconductors and simple metals with the use of empirical pseudopotentials [7]. In this approach, the total effective potential $V(r)$ in equation (2) was replaced by just a few adjustable terms in a Fourier expansion. In a more sophisticated approach a parametrized smooth model potential was used to replace that *ionic* part of $V_{\text{ext}}(r)$ in equation (2) which originates from the valence electrons only. The “ionic” parameters were adjusted to fit experimental band energies in a fully self-consistent calculation. The charge density given by the nodeless valence wave functions had no formal

connection to the true charge but was treated as the real valence charge in equation (2).

The formal justification for the use of pseudopotentials was initially based upon the orthogonalized-plane-wave (OPW) method [8]. The approach yields non-empirical pseudopotentials which are non-local in the sense that each angular momentum component of the valence pseudo wave function about an atomic center feels a different potential. The wave functions of OPW-type pseudopotentials have, however, the problem, that the normalized pseudo wave functions have incorrect amplitudes outside the core.

The problem is overcome by the concept of norm-conserving pseudopotentials [9]. For constructing these potentials one starts with a "reference" atom for which one has a self-consistent local density calculation, including core states at hand. A pseudo wave function for any valence state of the atom need have just *two* properties: it should be nodeless, and it should, *when normalized*, become identical to the true valence wave function beyond some core radius R_c (see Fig. 1). Such a function can be constructed in arbitrarily many ways. For any one pseudo wave function, the radial Schrödinger equation can be inverted to yield a pseudopotential which has this function as its eigenfunction at the correct eigenvalue. By this construction, it is clear that the pseudopotential and full potential are identical beyond R_c and that inside R_c the pseudopotential correctly simulates the scattering properties of the full potential at the eigenvalue energy and for the particular angular momentum under discussion. Moreover, it can be shown that the ionic (i.e., unscreened) portion of such "norm-conserving" pseudopotentials is *transferable* without first-order error to situations other than the atomic reference state. Such situations are e.g., molecules, solids or excited atomic configurations. A set of these pseudopotentials for all elements in the periodic table (H^1 through Pu^{94}) has recently been prepared [10]. For illustration the ionic pseudo potentials and wave functions are shown for Si in Fig. 1.

c) The quantitative solution of equation (2) for localized or deep defects remains a difficult problem even after electron-electron and electron-ion interactions are approximated as discussed in the previous paragraphs. I shall here describe the LCAO Green's function method as it has been used for quantitative calculations since several years [11, 12]. The electronic structure of the localized defect is described in the one-electron approximation by a Schrödinger equation of the form

$$(H_0 + U)\psi(r) = E\psi(r), \quad (3)$$

where H_0 is the Hamiltonian of the perfect crystal and U is the additional potential due to the defect. U is large but localized. The eigenfunctions of H_0 are the Bloch states of the perfect crystal and from these one can construct the perfect-crystal Green's function

$$\begin{aligned} G_E^0(r, r') &\equiv (E - H_0)^{-1} \\ &= \sum_n \int_{BZ} d^3k \frac{\psi_n(k, r) \psi_n^*(k, r')}{E - E_n(k)} \end{aligned} \quad (4)$$

The Green's function for the defect crystal $G_E(r, r') \equiv (E - H)^{-1}$ is related to the unperturbed G_E^0 by Dyson's equation

$$G = G^0 + G^0 U G, \quad (5)$$

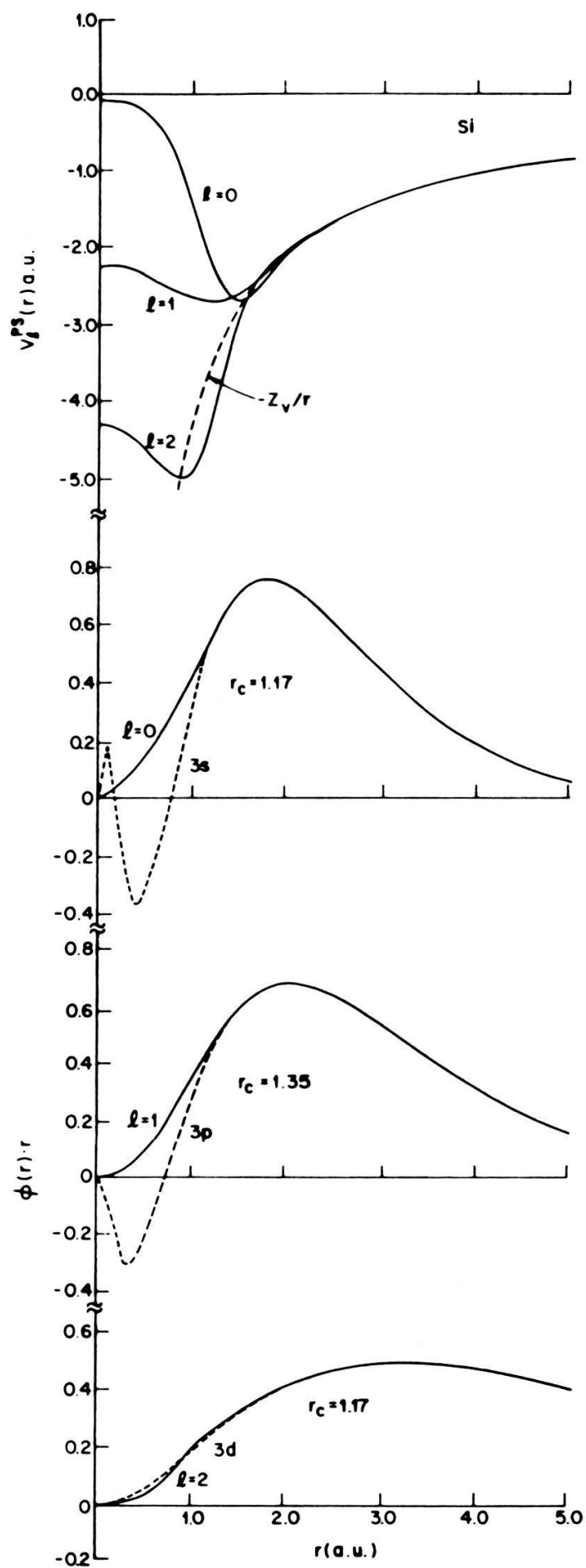


Figure 1
Norm-conserving ion-core pseudopotentials and wavefunctions for silicon.

The wave functions are expanded as linear combinations of localized Gaussian orbitals. The centers and shapes of the orbitals are chosen to correspond to the location and chemical identity of the atoms making up both the perturbed and unperturbed crystals. Both G^0 and G can be expressed in terms of these localized orbitals as $G_E^0(r, r') = \sum_{mm'} \psi_m(r) G_{mm'}^0 \psi_{m'}(r')$ and similarly for G . The choice of the orbital set $\{\psi\}$ is of crucial importance and allows the practitioner of the method much flexibility. Past experience has shown that using physical intuition one can select an optimal minimum set, which yields reliable numerical solutions of equation (2) with affordable computational effort. Using the orbital set $\{\psi\}$, Dyson's equation (5) becomes a matrix equation which can be solved for bound- and scattering states. The change in the state charge density is obtained for any energy E as

$$\Delta\rho_{mm'}(E) = \text{Im} [G_{mm'}(E) - G_{mm'}^0(E)] \quad (6)$$

The total charge density (with or without defect) requires the integration of $\text{Im} G_{mm'}(E)$ (or $G_{mm'}^0(E)$) over all occupied scattering and bound states. Once $\rho^0(r)$ and $\rho(r)$ are known with sufficient accuracy, defect total energies can *in principle* (as difference energies) be calculated from equation (1). *In practice* this task has turned out to be rather difficult and only very recently have total configurational energies been obtained within the Green's function scheme [13, 14, 15]. In addition to calculating total energies, much qualitative insight can be gained by studying spectral changes. Particularly instructive is the change in state density induced by the defect, which combined with real-space charge density changes yields much information on bonding around defects.

IV. The vacancy in silicon

While not of direct technological importance the vacancy in silicon is one of the most studied deep level defects and both theorists and experimentalist consider its physics as prototypical. The originally accepted picture of the vacancy, which is mainly due to the work of Watkins [16] is based on the underlying model is the Coulson-Kearsley defect molecule [17] model, where attention is focused on those orbitals in the crystal which are most perturbed by removal of the single atom to form the vacancy. As is illustrated in Fig. 2, there are four such orbitals, one on each of the four atoms nearest the vacancy and each associated with one of the four valence bonds broken by removal of the central atom. One-electron molecular orbitals are constructed as linear combinations of the four broken bond orbitals a , b , c , and d , associated with the atoms A , B , C , and D , respectively. Four such independent molecular orbitals can be constructed. The completely symmetric combination (A_1) is expected to be lowest in energy because it is nodeless. The other three are partner functions for a three-dimensional representation (T_2) of the T_d symmetry group of the undistorted vacancy. The Green's function calculations of the electronic states of the undistorted silicon vacancy shows that the threefold-degenerate T_2 level lies in the gap and that the A_1 state, or the resonance to which it gives rise, is located about 1 eV below the top of the valence band.

Qualitative but physical insight can be gained by inspecting the change distribution of valence electrons. Shown in Fig. 3 are contour plots of the total

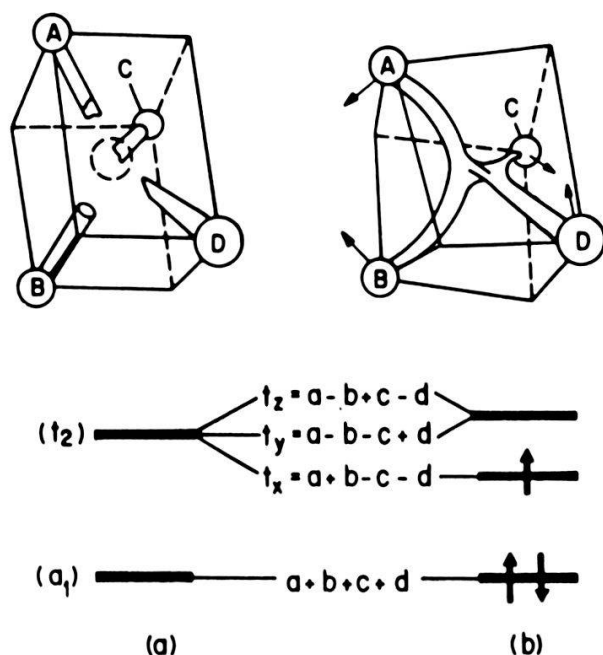


Figure 2

One-electron orbitals associated with the lattice vacancy: (a) undistorted, in tetrahedral symmetry; (b) after Jahn–Teller lattice distortion into a tetragonal symmetry.

unperturbed silicon charge (top) and the total charge in the presence of a vacancy (middle) clearly exhibiting the disappearance of bonding charge with the removal of an atom. This situation is very reminiscent of that of the (111) surface of silicon which also shows a “smeared out” and rounded charge distribution which decays rapidly into “vacuum.” The difference between the two densities, shown in the bottom panel is rather short-range and essentially confined to a cavity terminated by the nearest-neighbor atoms. This is in contrast to the behavior of individual states which can be quite extended (see Fig. 4). The fast “healing” of a perturbation has also been found for semiconductor surface systems and is one of the fundamental concepts underlying the present formalism.

We now return to the question of occupying the vacancy states in the defect molecule picture. For the vacancy to be e.g., in the doubly positively charged state V^{++} , two electrons must be distributed among the four states. They go into the A_1 state (or that resonance) with their spins paired leaving the deep level in the gap empty. For the singly positively charged state V^+ an extra electron has to be added into the T_2 level, a situation which, because of the orbital degeneracy, is unstable with respect to Jahn–Teller distortions. The type of distortion, as inferred from EPR experiments [16] which drops the energy of the T_x state and raises the T_y and T_z energy *without* splitting them, is illustrated in Fig. 2(b). It is tetragonal, with a $\langle 100 \rangle$ axis, and of D_{2d} symmetry. For the vacancy to be in its neutral state, V_0 , an additional electron is needed. This too goes into the T_x state, further increasing the amount of tetragonal distortion and pairing the spins. Experimental support for this picture is provided by Watkins’ EPR experiments [16], out of which has also emerged a tentative level scheme.

The picture has been modified and completed by our Green’s function calculations [18]. The calculations predict the stability of the doubly positively charged state of the vacancy V^{++} , a state which, being EPR invisible, has never

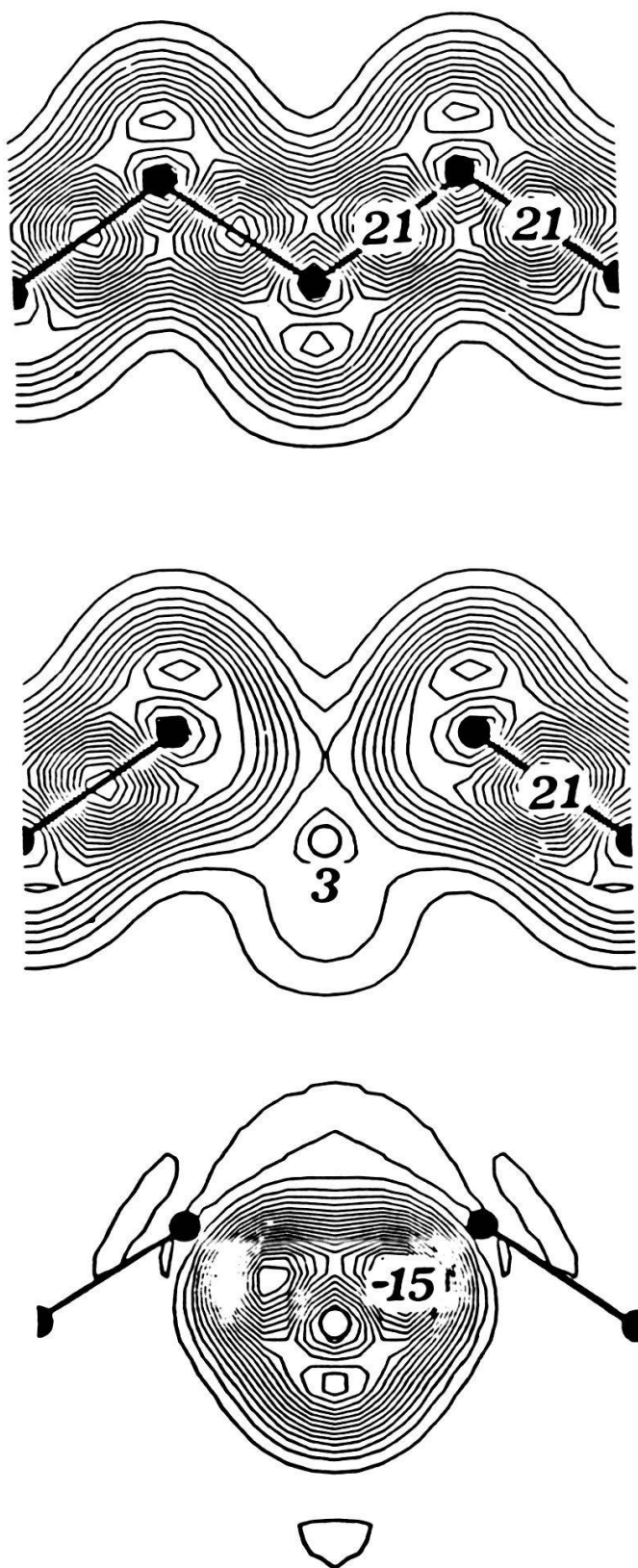


Figure 3
Contour plots of the unperturbed (1), perturbed (2) and total change (3) of charge densities induced by a silicon vacancy. Units are electrons/Si unit cell.

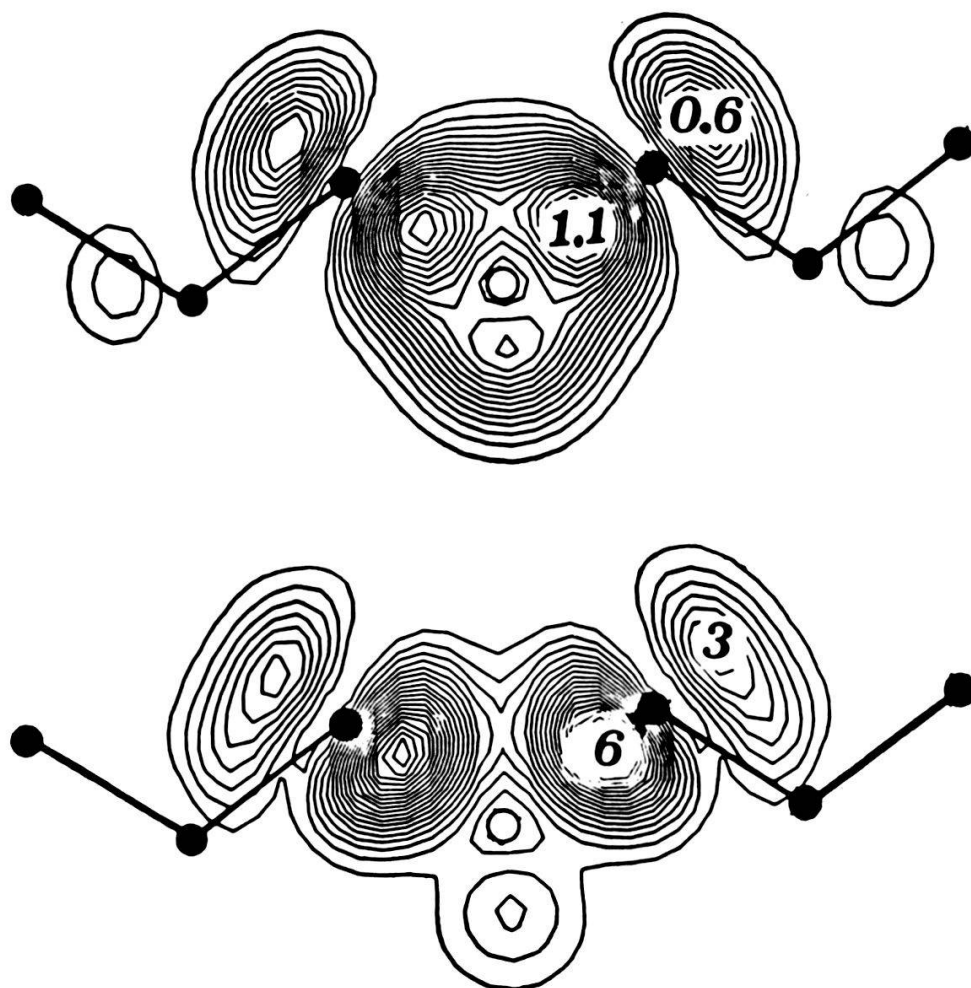


Figure 4

Charge contour plots of the A_1 resonance (top) and the T_2 bound state of the silicon vacancy.

been directly observed nor previously considered. Second, the calculations predict that the states V^0 , V^+ , and V^{++} form an “Anderson negative-effective- U system,” by which is meant that a level is associated with an *two-electron* transition between V^0 and V^{++} . This is unusual, because normally one would expect that electron–electron repulsion requires an extra energy, call it U , to add a second electron to a singly occupied state. Thus, as the Fermi energy is raised, the sequence of *expected* equilibrium states would be V^{++} , V^+ , and V^0 . The essence of Anderson’s “effective-negative- U ” idea, however, is that the energy-lowering structural Jahn–Teller distortion is sufficiently enhanced by the presence of a second electron that the energy gain more than compensates the e – e repulsive energy cost, U . In this case, a second electron will rapidly follow the first one on or off the center. The parameters we have calculated suggest that the transition induced by a change of Fermi energy is between equilibrium states V^0 and V^{++} , while V^+ is *never* the stable state of lowest energy.

It is appropriate to ask whether a negative U is a rare pathological situation or one to be met frequently. A simple scaling argument, familiar from polaron theory, gives some insight into this question. Let us regard the localization length of the defect as a characteristic coordinate. Then $U \sim 1/R$ scales like a typical Coulomb energy and the Jahn–Teller energy $\hat{E}_{JT} \sim -1/R^3$ scales like a “contact”

term which is directly proportional to the amount of charge in the defect level driving the Jahn–Teller distortion. It follows from this argument that for large R , i.e., for delocalized centres $U_{\text{eff}} > 0$ while increasing localization tends to reverse the sign of U_{eff} . There is, however, a cutoff for small R -values, roughly equal to the interatomic distance when the electron–lattice coupling becomes inoperative and the Coulomb repulsion becomes again dominant. Thus, if at all, U_{eff} could become negative for intermediate localization and then it depends on the “material parameters” U and $E_{JT} = V^2/2k$. A soft lattice (small k) favors a negative U_{eff} , so do a large electron–phonon coupling constant V and a small Coulomb repulsion U . The latter two are, however, counteracting each other in the sense that dielectric screening decreases both of them.

It can thus be regarded as a rather rare “coincidence” that our calculations predicted a negative U_{eff} (by ≈ 0.13 eV) for the silicon vacancy [18]. In fact, due to the numerical uncertainties in our estimates, the situation remained unsettled until in a very ingenuous experiment, Newton *et al.* unambiguously determined the negative U character of the silicon vacancy [19]. Few other point defect systems in semiconductors are known to be negative U systems.

V. Enhanced migration of aluminum in silicon

The migration of interstitial atoms in semiconductors is a long standing and fascinating problem. In particular the phenomenon of capture – or recombination enhanced migration has been recognized as an important feature of defect reactions and device degradations [20–23]. The mechanism for this enhancement is, generally speaking, that part of the energy stored in electrons and holes (i.e., about E_g /per pair) can be released upon carrier capture or recombination and can thus supply part of the energy necessary for the defect to make a diffusional jump. Various theoretical models have been proposed for this mechanism [24, 25] but a basic understanding is only slowly emerging.

There is detailed experimental information available for a particular case, namely for the migration of Al in silicon [25] which we shall discuss here. Interstitial Al is produced by electron irradiation of Al (substitutional) doped p -type silicon at room temperature. The defects can be monitored by DLTS and EPR techniques. The results are compatible with a $E(+/+ +)$ level at $\approx E_V + 0.17$ eV, exhibiting tetrahedral symmetry. With no free carriers present the defect diffuses with an activation barrier of ~ 1.2 eV while in the presence of carriers this barrier is lowered to ~ 0.27 eV. At the same time the pre-exponential rate drops by a factor of 10^7 . This remarkable result is shown in Fig. 5. The process is very energy efficient, considering a 0.9 eV barrier lowering in a material with a 1.1 eV bandgap.

We have recently attempted [15, 26] to explain these findings by developing a detailed model based on Green’s function calculations. To obtain the quantities needed to evaluate the diffusion barriers we consider Al at two different interstitial sites, the tetrahedral (T_d) site which, according to the experimental results is probably the energy minimum along the diffusion path and the hexagonal (D_{2d}) site which is either a maximum or more likely the highest saddle point along the diffusion path. Figure 6 shows calculated charge–density contours for tetrahedral Al^{++} . The interstitial is fourfold coordinated. It attempts to establish tetrahedral

bonds to its neighboring atoms, thereby slightly weakening their preexisting bulk-like bonds. This is quite remarkable since the four surrounding Si atoms are now 5-fold coordinated. A deep A_1 bound state in the gap and a strong T_2 resonance at the edge of the conduction band correspond to mainly Al p -like states of nonbonding character. The A_1 bound state gives rise to an electrical level $E(+ / + +) \approx E_v + 0.2 \text{ eV}$ in good agreement with the measurements. Virtually no lattice relaxations are calculated to occur for Al in the tetrahedral site. However, the stiffness of some local phonon modes is increased by up to 40%.

As one moves the interstitial atom from the high-symmetry tetrahedral site to

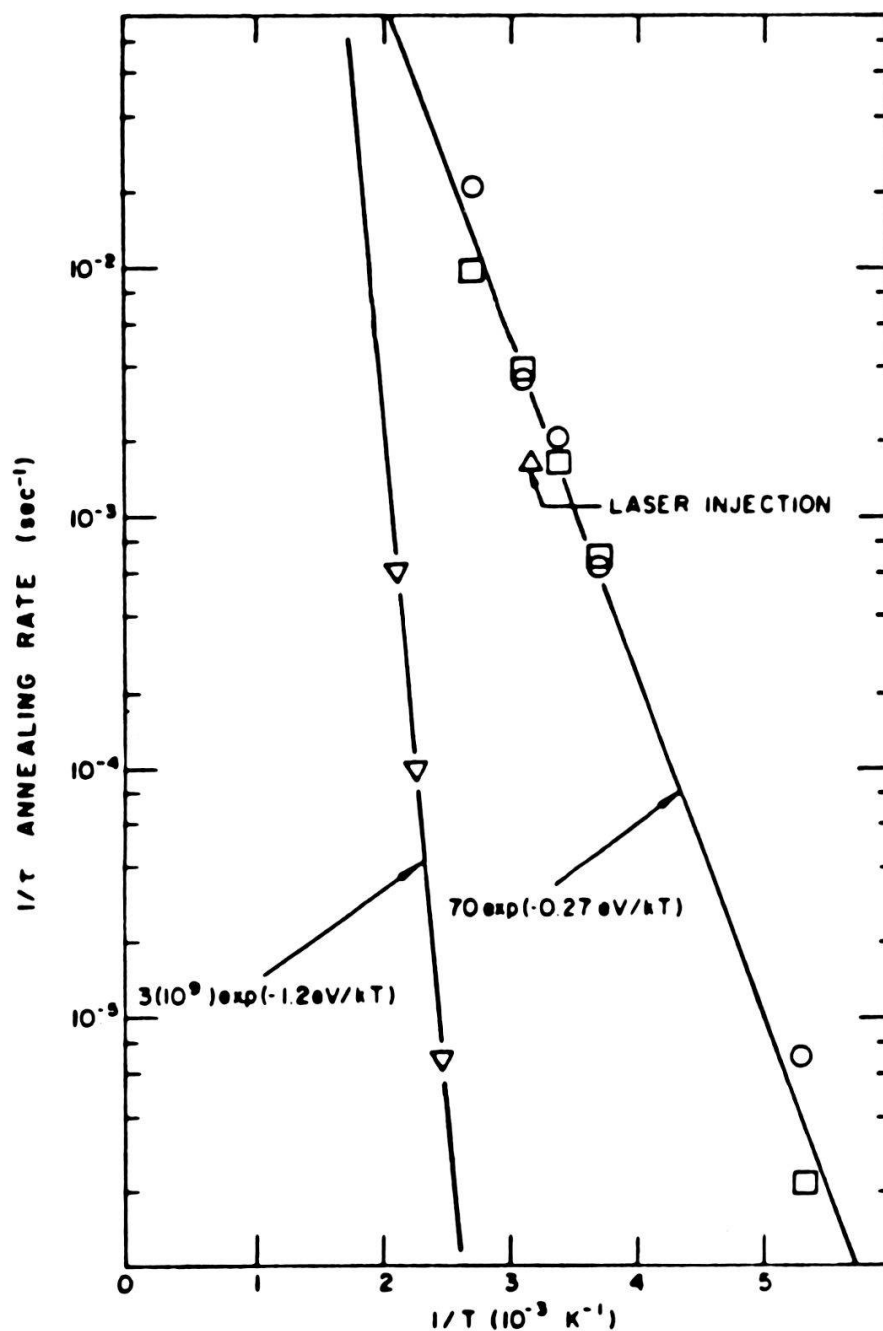


Figure 5

Experimental temperature dependence of the annealing rate of the interstitial Al defect in silicon. Two curves are shown: with no free carriers present (∇) and with free carriers present either injected in a junction (\square , \circ) or by laser light (∇) (from Ref. 25).

the lower-symmetry hexagonal site, the threefold degenerate T_2 resonance in the conduction band splits into a twofold degenerate resonance which rises and a onefold degenerate state which drops into the gap. The new deep state in the gap can be occupied by zero, one, or two electrons, creating two additional electrical levels.

The calculated charge densities for hexagonal Al^{++} are shown in Fig. 7. Insertion of an Al atom at the hexagonal site creates a local environment of high

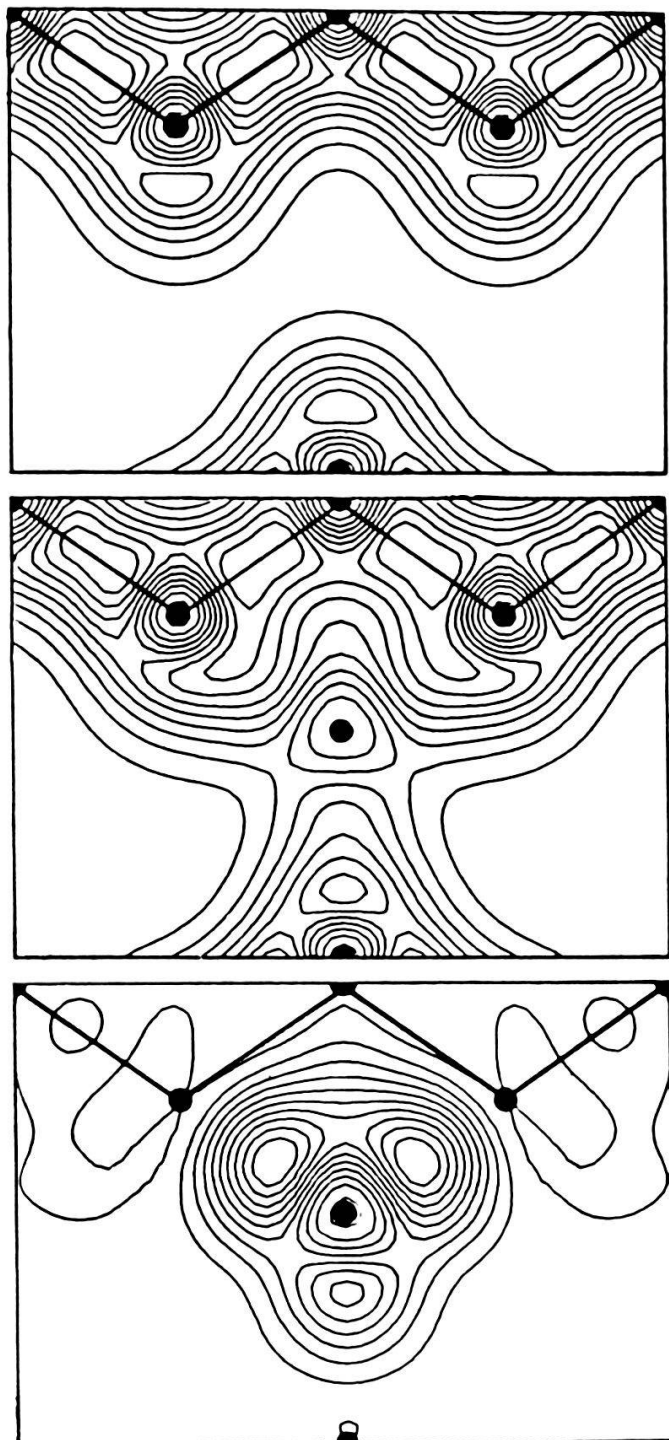


Figure 6

Charge density contours in a (100) plane calculated with the Green's function technique for perfect Si (top) and for Si with an interstitial Al atom in the tetrahedral site (middle). The charge difference between the two is shown in the bottom figure.

and remarkably constant, i.e., ‘metallic,’ electron density. The six Si atoms surrounding the Al interstitial show a sizeable outward breathing distortion ($\approx 6\%$).

The calculated strong spectral changes between the T_d and D_{3d} sites suggest their involvement in the migration enhancement process. We propose on the basis of our calculations a new model for the enhanced migration of interstitial Al. The migration path for Al presumably originates at a stable tetrahedral site and lies along the nearly charge-free channels, while the hexagonal site is presumably a

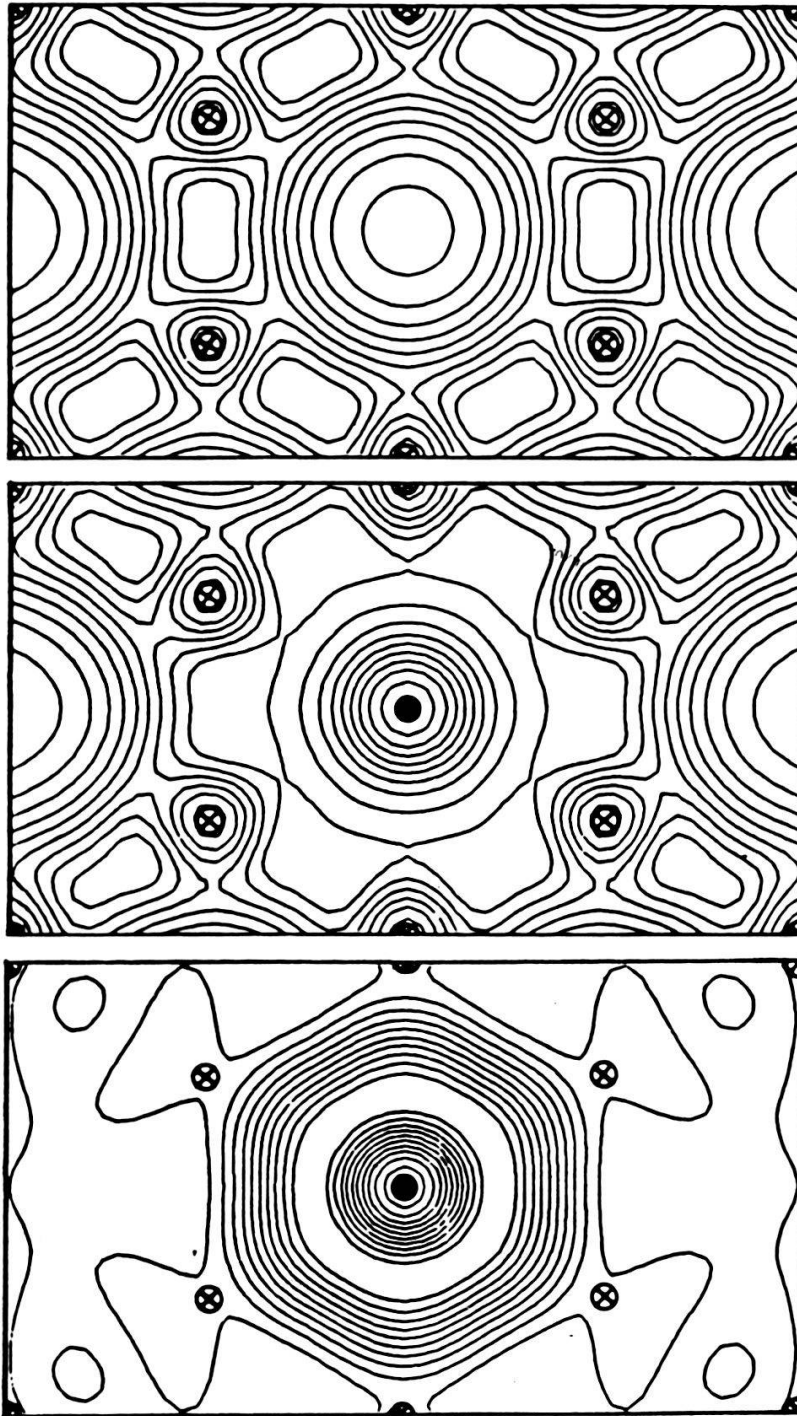


Figure 7

Charge density contours near the hexagonal site in silicon, displayed in a (111) plane. Perfect Si is shown on top, Si with an interstitial Al atom in the middle and the difference charge at the bottom.

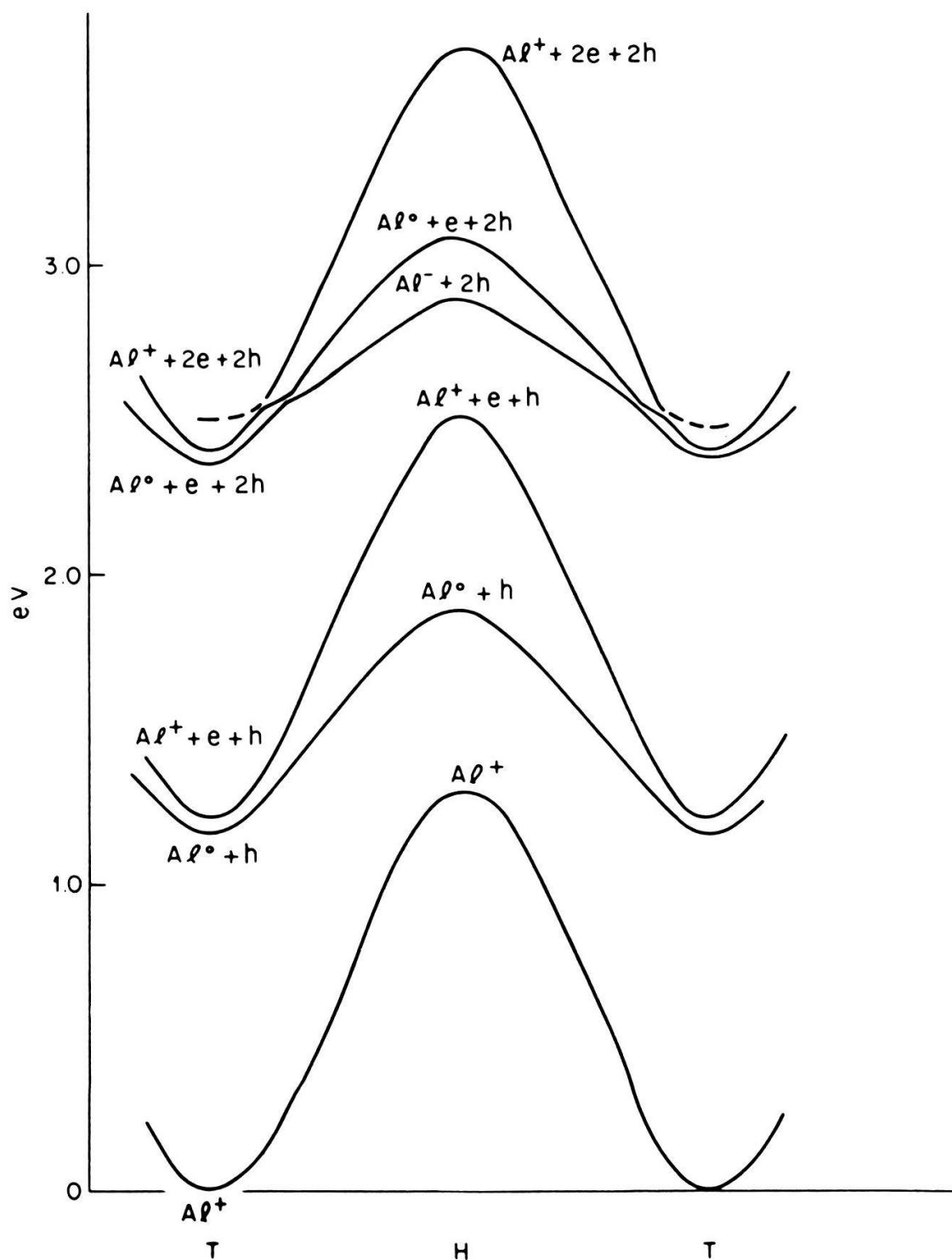


Figure 8

Configuration coordinate diagram for the total energy variation of Al diffusing along the channel in silicon. The lower curve corresponds to the diffusion of Al^+ without free carriers present. The upper curves, shifted by E_G and $2E_G$ respectively corresponds to Al^+ plus free electrons and holes. The shallow state for the tetrahedral site (T), Al^0 becomes a deep state for the hexagonal site (H). A second electron can be captured into the deep state resulting in Al^- . The set of curves corresponds to the barrier values calculated in Ref. 15.

saddle point on this path. There is a sizeable energy barrier (measured as 1.27 eV in *p*-type Si and calculated as $V_B^+ = 1.3 \pm 0.5$ V) associated with unassisted migration (see lowest curve in Fig. 8). This barrier results mainly from the drastic changes in bonding configuration as illustrated by the changes in the local charge density, and is also modified by different elastic distortions.

Under electron injection, all the tetrahedral Al^{++} converts to Al^+ at low currents. The positively charged Al^+ can bind another electron in a shallow effective-mass-like state Al^0 . The strong T_2 resonance near the conduction-band minimum splits and a state drops into the gap as the Al vibrates thermally from the tetrahedral position towards the hexagonal one. This allows the effective mass like electron to be localized in the vicinity of the Al interstitial lowering the barrier by about 0.6 eV. A second electron can be trapped leading to Al^- and a further barrier lowering of 0.2 eV. Our calculations show that the shallow-deep transition of these two electrons acts as a driving mechanism to help move the Al atom along the tetrahedral-hexagonal path (see Fig. 8).

Apart from the remarkably high barrier lowering which according to our model can be obtained by trapping two electrons, a drastic drop in the pre-exponential factor for the recovery rate of the defect has also been observed (see Fig. 5). In fact the factor drops from $3 \cdot 10^9 \text{ sec}^{-1}$ to 70 sec^{-1} indicating very different mechanism limiting the diffusion in the two cases. The value of $3 \cdot 10^9 \text{ sec}^{-1}$ is typical for a thermal process i.e., the lattice vibrational frequency ($\sim 10^{13} \text{ sec}^{-1}$) divided by the number of migrational jumps required before the defect becomes trapped ($\sim 10^4$). The value of 70 sec^{-1} can be explained on the basis of thermal vibrations only if a very small concentration of trapping centers is assumed. This is, as discussed in Ref. 27, compatible with a two electron capture changing the charge state of the diffusing atom from + to -.

VI. Conclusions and summary

The quantum theory of defects has shown remarkable activity in the past 5–10 years. This activity partly follows and partly parallels successful quantum-mechanical descriptions of the chemical bonding in bulk crystals and near surfaces. The impressive advances in these fields are results of successful marriages between conceptionally clear and simple, yet quantitative procedures: the Density Functional Theory, the Pseudopotential Method, and for the study of defects, the Green's function technique; However, in spite of the impressive amount of work done there still remain many fundamental problems to be explained, which makes this field attractive and interesting.

Acknowledgment

This article is dedicated to Mani on his 60th birthday. I am very thankful for his guidance and friendship which I have enjoyed since my student time.

I also would like to thank Gene Baraff for his contributions to our long-time collaboration on the subjects discussed in this paper.

REFERENCES

- [1] P. HOHENBERG and W. KOHN, *Phys. Rev.* **136**, B864 (1964).
- [2] W. KOHN and L. J. SHAM, *Phys. Rev.* **140**, A1133 (1965).
- [3] A. R. WILLIAMS and U. VON BARTH, in "Theory of the Inhomogeneous Electron Gas", Ed. S. Lundquist and N. H. March (New York, 1983).
- [4] O. GUNNARSSON and R. O. JONES, *Physica Scripta*, **21**, 394 (1980).
- [5] W. KOHN and P. VASHISTA, in "Theory of the Inhomogeneous Electron Gas", Ed. S. Lundquist and N. H. March (New York, 1983).
- [6] M. SCHLÜTER and L. J. SHAM, *Physics Today* **2**, 36 (1982).
- [7] For a review, see M. L. COHEN and V. HEINE, in *Solid State Physics*, vol. 24, p. 38 Ed. H. E. Ehrenreich, F. Seitz and D. Turnbull (New York, 1970) and V. Heine and D. Weaire, *ibid.* p. 249.
- [8] C. HERRING, *Phys. Rev.* **52**, 1169 (1940).
- [9] D. R. HAMANN, M. SCHLÜTER and C. CHIANG, *Phys. Rev. Lett.* **43**, 1494 (1979).
- [10] G. B. BACHELET, D. R. HAMANN and M. SCHLÜTER, *Phys. Rev.* **B26**, 4199 (1982).
- [11] G. A. BARAFF and M. SCHLÜTER, *Phys. Rev. Lett.* **41**, 892 (1978).
- [12] J. BERNHOLC, N. LIPARI and S. T. PANTELIDES, *Phys. Rev. Lett.* **41**, 895 (1978).
- [13] G. A. BARAFF and M. SCHLÜTER, *Phys. Rev. B*, **28**, 2296 (1983).
- [14] R. CAR, P. J. KELLY, A. OSHIYAMA and S. T. PANTELIDES, *Phys. Rev. Lett.* **52**, 1814 (1984).
- [15] G. A. BARAFF and M. SCHLÜTER, *Phys. Rev.* **B30**, 3460 (1984).
- [16] G. D. WATKINS, in *Point Defects in Solids*, vol. 2, p. 333, Ed. J. H. Crawford Jr. and L. M. Slifkin (New York, 1975).
- [17] C. A. COULSON and M. J. KEARSLEY, *Proc. Roy. Soc. London Sci.* **A241**, 433 (1957).
- [18] G. A. BARAFF, E. O. KANE and M. SCHLÜTER, *Phys. Rev.* **B21**, 5662 (1980).
- [19] J. L. NEWTON, A. P. CHATTERJEE, R. D. HARRIS and G. D. WATKINS, *Proc. 12th Intl. Conf., Defects Semicond.*, p. 219, Ed. C. A. J. Ammerlaan, Amsterdam (1983).
- [20] L. C. KIMERLING, in *Defects and Radiation Effects on Semiconductors*, IOP Conference Proceedings No. 26, p. 56, Ed. J. H. Albany (London, 1979).
- [21] G. D. WATKINS, J. R. TROXELL and A. P. CHATTERJEE, in *Defects and Radiation Effects in Semiconductors*, IOP Conference Proceedings No. 46, p. 16, Ed. J. H. Albany (London, 1979).
- [22] D. V. LANG, *Ann. Rev. Mater. Sci.* **12**, 377 (1982).
- [23] P. M. PETROFF, in *Semiconductors and Insulators*, vol. 5, p. 307, (New York, 1983).
- [24] M. LANNOO and J. BOURGOIN, in *Point Defects in Semiconductors I*, Springer Series in Solid State Sciences No. 22 (New York, 1981).
- [25] J. R. TROXELL, A. P. CHATTERJEE, G. D. WATKINS and L. C. KIMERLING, *Phys. Rev.* **B19**, 5336 (1979).
- [26] G. A. BARAFF, M. SCHLÜTER and G. ALLAN, *Phys. Rev. Lett.* **50**, 739 (1983).
- [27] M. SCHLÜTER, *Proc. 13th Intl. Conf. Defects Semicond.*, Coronado 1984, in print.